Depth-variant blind restoration with pupil-phase constraints for 3D confocal microscopy

Saima Ben Hadj, Laure Blanc-Féraud, Engler Gilbert

Depth-variant blind restoration with pupil-phase constraints for 3D confocal microscopy

Saima Ben Hadj [1], **Laure Blanc-Féraud** [1], **and Gilbert Engler** [2]

[1] Morphème research group - I3S/INRIA/CNRS/IBV/UNS,
2000, route des Lucioles, 06903 Sophia Antipolis Cedex, France
[2] Unit IBSV, INRA, 06903 Sophia Antipolis, France

E-mail: Saima.Ben_Hadj@inria.fr, Laure.Blanc_Feraud@inria.fr, Gilbert.Engler@sophia.inra.fr

Abstract. Three-dimensional images of confocal laser scanning microscopy suffer from a depth-variant blur, due to refractive index mismatch between the different mediums composing the system as well as the specimen, leading to optical aberrations. Our goal is to develop an image restoration method for 3D confocal microscopy taking into account the blur variation with depth. The difficulty is that optical aberrations depend on the refractive index of the biological specimen. The depth-variant blur function or the Point Spread Function (PSF) is thus different for each observation. A blind or semi-blind restoration method needs to be developed for this system. For that purpose, we use a previously developed algorithm for the joint estimation of the specimen function (original image) and the 3D PSF, the continuously depth-variant PSF is approximated by a convex combination of a set of space-invariant PSFs taken at different depths. We propose to add to that algorithm a pupil-phase constraint for the PSF estimation, given by the the optical instrument geometry. We thus define a blind estimation algorithm by minimizing a regularized criterion in which we integrate the Gerchberg-Saxton algorithm allowing to include these physical constraints. We show the efficiency of this method relying on some numerical tests.

1. Introduction

Confocal laser scanning microscopy allows to observe in three dimensions (3D) biological living specimens, at a resolution of few hundred nanometers. However, 3D images coming from this system are mainly affected by two types of distortion: a depth-variant (DV) due to the refractive index variation between the different mediums composing the system as well as the specimen, and a Poisson noise due to the photon counting process at the sensor. The knowledge of the Point Spread Function (PSF) is crucial for the restoration of these images. Theoretical models for the 3D PSF computation were previously developed in the literature based on the geometrical optics. For example, we use the model described in [3, 5] for the simulation of blurred confocal microscopy images. Nevertheless, this model relies on the knowledge of some physical acquisition parameters which are inaccessible in practice such as the refractive index of the biological specimen. The estimation of the 3D DV PSF is an important problem which is highly under-determined.

In our previous work, we considered an approximation of the 3D DV PSF by a convex combination of a set of space-invariant (SI) PSFs taken at different depths [1]. A method for the joint estimation of the specimen function (the original image) and the 3D DV PSF is proposed

in [1] and summarized in section 2.

In this article, we propose to add an additional constraint on the PSF coming from modeling the optical instruments. In fact, the PSF of confocal microscopy can be computed from the magnitude of a complex function known as the *complex valued-amplitude PSF* [3, 5]. The shape and the support of this complex function are given in the Fourier domain by the numerical aperture of the optical system (this latter is known since it is fixed by the system manufacturer) [5]. We propose to incorporate these constraints in the joint image and PSF estimation algorithm presented in [1]. For that, we use the Gerchberg-Saxton algorithm [4] which allows to impose these constraints on the PSF (i.e. constraints on the pupil phase).

This article is organized as follows : We first recall the DV PSF model and the joint estimation algorithm proposed in [1]. We then describe the constraints to be imposed on the estimated PSF, arising from the optic modeling. We present the proposed algorithm for incorporating these constraints in the estimation algorithm. We finally present some numerical results showing the interest of these constraints.

2. Joint image and PSF estimation algorithm

Let $f,\, g : \mathcal{I} \subset \mathbb{N}^3 \rightarrow \mathbb{R}^+$ be two functions denoting respectively the original and the degraded discrete 3D images ($\mathcal{I}$ being the image support). The forward degradation model is given by the following Poisson statistics: $g \sim \mathcal{P}\left(\widetilde{H}\left(f\right) + b_g\right)$ where $b_g > 0$ is a strictly positive constant modeling the background noise, coming from the specimen auto-fluorescence or light scattering. b_g is assumed to be known since it can be estimated from a dark region which does not contain the object. The DV blur operator $\widetilde{H}$ can be modeled as follows [1]: $\widetilde{H}\left(f\right) = \sum\limits_{1 \leq i \leq M} h_i * \left(\psi_i . f\right)$ where h_i, $i = 1,\, ...,\, M$ is a set of SI PSFs taken at different depths and $\psi_i : \mathcal{I} \rightarrow [0,\, 1]$, $i = 1,\, ...,\, M$ is a set of weighting functions such that $\sum\limits_{1 \leq i \leq M} \psi_i(x, y, z) = 1,\, \forall (x, y, z) \in \mathcal{I}$. The choice of these weighting functions is discussed in [3] where it is shown that piecewise-linear functions are sufficient to obtain a good restoration. We thus consider that $\psi_i\left(x, y, z\right)$ are varying along (OZ) axis and constant along (OX) and (OY) axis. For fixed weighting functions, the image and the PSFs can be estimated by minimizing the following criterion [1]:

$$\begin{aligned} J\left(f,\, h^1,\, ...,\, h^M\right) = & \sum_{(x,y,z) \in \mathcal{I}} \left[\widetilde{H}\left(f\right)(x, y, z) - g(x, y, z)\, log\, \left(\widetilde{H}\left(f\right)(x, y, z) + b_g\right)\right] \\ & + \alpha\, \left\|\nabla f\right\|_1 + \sum_{1 \leq i \leq M} \beta_i\, \left\|\nabla h_i\right\|_2^2 \end{aligned} \tag{1}$$

The first term is the data fidelity term arising from the Poisson statistic. The second term defines the total variation for the image smoothing while preserving edges. The last term promotes regular and spread PSFs in order to capture all the blur of the observed image in the PSF. α and β_i, $i = 1,\, ...,\, M$ are regularization parameters. We define the set of admissible images as follows: $C_f = \{f; f \geq 0;\, \left\|f\right\|_1 = \left\|g - b_g\right\|_1\}$ and the set of admissible PSFs as follows: $C_h = \{h; h \geq 0; \left\|h\right\|_1 = 1; supp\left(h\right) \subset B\}$, $B \subset \mathcal{I}$ being the PSF support. The joint image and PSF estimation can be performed as in [1] by alternatively minimizing the criterion (1) w.r.t f and $h_i, i = 1,\, ...,\, M$, the constraints of C_f and C_h being involved using a fast scaled gradient projection (SGP) [2]:

(i) Object estimation using SGP [2]: $\hat{f}^{(k+1)} = \underset{f \in C_f}{\arg\min}\, J\left(f,\, \hat{h^1}^{(k)},\, ...,\, \hat{h^M}^{(k)}\right)$

(ii) PSF estimation using SGP [2]: For $i = 1,\, ...,\, M$, $\hat{h_i}^{(k+1)} = \underset{h_i \in C_h}{\arg\min}\, J\left(\hat{f}^{(k+1)},\, \hat{h^1}^{(k)},\, h_i,\, ...,\, \hat{h^M}^{(k)}\right)$

It is worth stressing that the minimized criterion is non-convex w.r.t all the variables $(f, h^1, ..., h^M)$ but it is convex w.r.t. each of the variables separately. Thus the proposed algorithm seeks for a local minimum which depends on the PSF initialization. In our tests, the PSFs are initialized from the theoretical PSF model that we present in the following section by setting approximately its physical parameters (namely the refractive index of the immersion medium and the sample).

3. Pupil phase constraints for the PSF estimation

Since the problem of blind restoration is under-determined, it is important to inject as much information as possible on the unknown variables. In particular, the PSF comes from modeling the optical instrument and can be written as follows [3, 5]:

$$h_i\left(x,\, y, z\right) = \left|h_{Ai}\left(x,\, y, z\right)\right|^4 \tag{2}$$

where h_{Ai} is a complex function $h_{Ai}(x, y, z) \in \mathbb{C}$ called *complex valued-amplitude PSF* or *coherent PSF*. In that model, excitation and emission wavelengths are assumed to be sufficiently close in such a way that their associated coherent PSFs could be considered of the same magnitude. Moreover, the pinhole diameter is assumed to be sufficiently small in such a way that it could be modeled by a Dirac distribution and thus does not appear in the PSF model (2). Furthermore, we have :

$$h_{Ai}\left(x,\, y, z\right) = TF_{2D}^{-1}\left(P_i\left(k_x,\, k_y, z\right)\right) \tag{3}$$

where $P_i\left(k_x,\, k_y, z\right) \in \mathbb{C}$ is the 2D pupil function computed for each Z-slice, TF_{2D}^{-1} is the 2D inverse Fourier transform, and k_x, k_y are the 2D frequency coordinates. This pupil function can be decomposed into two terms:

$$P_i\left(k_x,\, k_y,\, z\right) = P_{ai}\left(k_x,\, k_y\right)\, P_d\left(k_x,\, k_y, z\right) \tag{4}$$

The term $P_d\left(k_x,\, k_y, z\right)$ models the defocus of the optical instruments and is assumed to be known since it is given by the system physical parameters [5]. The term $P_{ai}\left(k_x,\, k_y\right) \in \mathbb{C}$ models the aberrations affecting the wavefront when traveling through the different system mediums. It is unknown since it is related to the biological specimen. Note that the aberration term does not depend on the z coordinate while the defocus term depends on that coordinate, which allows us to introduce constraints on the PSF in the Fourier domain. The support C of the aberration term is a disk of radius given by the numerical aperture (NA) of the microscope: $C = \{(k_x,\, k_y) \in \mathbb{N}^2;\, \sqrt{k_x^2 + k_y^2} < \frac{2\pi}{\lambda}\, NA\}$. This model allows us to impose additional constraints on the PSF (shape and support).

4. Blind restoration with pupil phase constraints

To take into account the constraints given in section 3, we add to the previous algorithm (section 2) an additional step allowing to estimate the complex function h_{Ai}, by estimating in the Fourier domain the aberration term P_{ai}, the defocus term P_d is fixed by the acquisition system. In order to estimate the term P_{ai} from the PSF h_i, we propose to use the Gerchberg-Saxton algorithm which was successfully applied in [4] to wide field microscopy. The global estimation algorithm is the following, k being the iteration counter:

(i) Object estimation using SGP algorithm [2]: $\hat{f}^{(k+1)} = \underset{f \in C_f}{\arg\min}\, J\left(f,\, \hat{h^1}^{(k)},\, ...,\, \hat{h^M}^{(k)}\right)$

(ii) PSF estimation: For $i = 1,\, ...,\, M$, iterate the following steps:

(a) Estimation of the PSF using SGP [2]: $\hat{h_i}^{(k+1)} = \underset{h_i \in C_h}{\arg\min}\, J\left(\hat{f}^{(k+1)},\, \hat{h^1}^{(k)},\, h_i,\, ...,\, \hat{h^M}^{(k)}\right)$

(b) Estimation of the aberration term ${P_{ai}}^{(k+1)}$ from the PSF $\hat{h_i}^{(k+1)}$ using the Gerchberg-Saxton algorithm as described below.

(c) Compute the new PSF: $\hat{h_i}^{(k+1)}(x, y, z) = |TF_{2D}^{-1}\left(P_d\,(k_x,\, k_y, z)\, {P_{ai}}^{(k+1)}\,(k_x,\, k_y)\right)|^4$

Gerchberg-Saxton algorithm [4] allows the estimation of $P_{ai}^{(k+1)}$ by alternating constraints in the spatial domain (magnitude of h_{Ai} given by h_i) and in the frequency domain (the shape of h_{Ai} and the support of P_{ai} given by C) as follows:

(i) For each z-slice compute ${h_{Ai}}^{(k+1)}\,(x,\, y, z) = TF_{2D}^{-1}\left(P_d\,(k_x,\, k_y, z)\,.{P_{ai}}^{(k)}\,(k_x,\, k_y)\right)$

(ii) Replace the module of ${h_{Ai}}^{(k+1)}$ by $\sqrt[4]{\hat{h_i}^{(k+1)}}$

(iii) For each z-slice compute ${P_{aiz}}^{(k+1)}\,(k_x,\, k_y) = TF_{2D}\left({h_{Ai}}^{(k+1)}\,(x,\, y, z)\right) {P_d}^{-1}\,(k_x,\, k_y, z)$, then compute ${P_{ai}}^{(k+1)}$ as the average of these estimated aberration terms for different z-slices.

(iv) Project ${P_{ai}}^{(k+1)}$ in the set of function having their support included in $C = \{(k_x,\, k_y) \in \mathbb{N}^2;\, \sqrt{k_x^2 + k_y^2} < \frac{2\pi}{\lambda}\, NA\}$.

The convergence of the Gerchberg-Saxton was proved in [7]. The convergence of the proposed minimization algorithm under a set of constraints to a local minimum of J will be the goal of our future work. Numerical results show however a good behavior of such an estimation scheme.

5. Numerical experiments

We numerically generated a 3D image of a bead shell of thickness $400\,nm$ and of internal diameter of $5\,\mu m$. The image size is of $140 \times 140 \times 70$ voxels, the voxel size being $50\,nm$ along (Y, Y) axis and $140\,nm$ along Z axis. An (Y, Z) slice of that image is shown in figure 1 (b). We degraded this image by a DV blur (for each z-slice, we used a new 3D PSF calculated by the model described in [3, 5]) and a Poisson noise, the background noise is set to $b_g = 10^{-4}$ (see figure 1 (a)). Note that a high value of the background constant decreases the signal to noise ratio. We then restored this image using a combination of 3 PSFs. The regularization parameters are set by try/error as follows: $\alpha = 10^{-3}, \beta_1 = 4.\,10^4, \beta_2 = 5.\,10^5, \beta_3 = 5.\,10^5$. The automatic estimation of these parameters will be the goal of our future work [8]. The comparison of the estimated image and one of 3 PSFs (figures 1 (c) and (f)) with those obtained by an algorithm without the pupil phase constraint [1] (figures 1 (d) and (g)) and comparison with the true image and PSF (see figures 1 (a) and (e)) show the advantage of the proposed approach. Our method allows to constrain the shape of the PSF. Note that the lobe of the original PSF is shifted from its central plane due to spherical aberration effects (see figure 1 (e)). Nevertheless, the estimated PSFs (figures 1 (f) and (g)) are centered because this shift is actually not estimated by the proposed method, even when considering the pupil phase constraints. An interesting future work is to estimate the PSF shift by introducing a strong constraint about this parameter. For example, one can obtain an information about the true object position (i.e. an information about the shift parameter) from a diffractive tomography microscopy system which can be coupled with the confocal microscopy system [9].

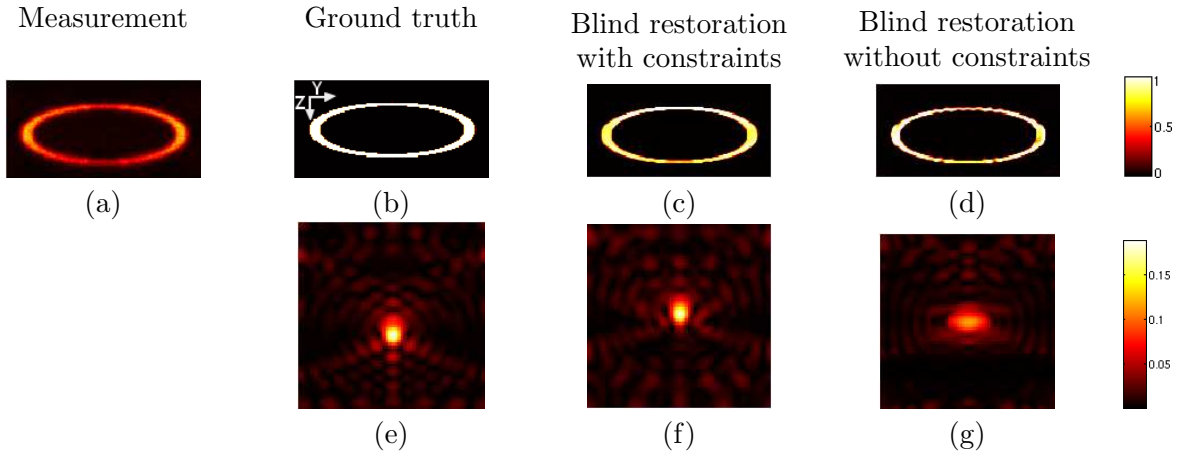

Figure 1. (Y, Z) of the (a) observation, the original image (b), the estimated image (c) and one of the 3 PSFs (f) using the proposed method, the estimated image (d) and one of the 3 PSFs (g) using the algorithm proposed in [1], the true PSF (e).

References

[1] S. Ben Hadj, L. Blanc-Fraud, G. Aubert, *Space Variant Blind Image Restoration*. Rapport de recherche INRIA 8073, September, 2012.

[2] S. Bonettini, R. Zanella, and L. Zanni. *A scaled gradient projection method for constrained image deblurring*. Inverse Problems, 2009, 25 : 015002.

[3] A. Egner, and S.W. Hell. *Aberrations in confocal and multi-photon fluorescence microscopy induced by refractive index mismatch*. Handbook of Biological Confocal Microscopy, 2006, 404–413.

[4] B.M. Hanser, M.G.L. Gustafsson, D.A. Agard, and J.W. Sedat. *Phase retrieval for high-numerical-aperture optical systems*. Optics letters, 2003, 28(10) : 801803.

[5] P.A. Stokseth. *Properties of a defocused optical system*. JOSA, 1969, 59(10) : 13141321.

[6] S. Yuan, and C. Preza. *3D fluorescence microscopy imaging accounting for depth-varying point-spread functions predicted by a strata interpolation method and a principal component analysis method*. SPIE, 2011, 19(23) : 23298-23314.

[7] J. R. Fienup. *Phase retrieval algorithms: a comparison*. Applied optics, 1982, 21(15) :2758–2769.

[8] X. Zhu, and P. Milanfar. *Automatic parameter selection for denoising algorithms using a no-reference measure of image content*. IEEE Transactions on Image Processing, 2010, 19(12) : 3116-3132.

[9] M. Sarmis, B. Simon, M. Debailleul, B. Colicchio, V. Georges, J.J. Delaunay, and O. Haeberle. *High resolution reection tomographic diffractive microscopy*. Journal of Modern Optics, 2010, 57(9) : 740-745.